Neutron and x-ray diffraction studies of a-C:N:H

1996 J. Phys.: Condens. Matter 8 4739

(http://iopscience.iop.org/0953-8984/8/26/006)

J. Phys.: Condens. Matter **8** (1996) 4739–4750. Printed in the UK

Neutron and x-ray diffraction studies of a-C:N:H

J K Walters†, R J Newport‡, W S Howells§ and G Bushnell-Wye‖

† Department of Physics and Astronomy, University College London, Gower Street, London WC1E 6BT, UK

‡ Physics Laboratory, The University, Canterbury, Kent CT2 7NR, UK

§ Neutron Division, CLRC Rutherford Appleton Laboratory, Didcot, Oxon OX11 0QX, UK

‖ CLRC Daresbury Laboratory, Daresbury, Warrington WA4 4AD, UK

Received 25 March 1996, in final form 2 May 1996

Abstract. The results of neutron and x-ray diffraction experiments performed on a range of nitrogen-doped amorphous hydrogenated carbon (a-C:N_x:H, where $x = 0$, 6, 8 and 10 at.%) samples are presented. Changes in the average bond lengths and bond angles are observed as the nitrogen content is varied; however, no qualitative structural differences are seen between the samples. Both CH and NH correlations are seen directly, and N–H bonds are shown to be favoured over C–H at the highest N concentration. Also for the sample with the highest N content, the data provide evidence for the presence of a small quantity of C≡N triple bonds, although this is not the dominant bonding environment of N. The data indicate that N incorporation may result in some transformation of sp^3 C sites to sp^2 sites, but there is no evidence for N inducing the formation of graphitic clusters, and the structure remains disordered overall.

1. Introduction

A complex problem in the study of amorphous materials is that of determining the relationship between the atomic-scale structure and the macroscopic properties of a material, the solution of which maintains amorphous materials in a position of both fundamental and technological interest. In fact, as novel materials continue to be generated, the range of questions only increases.

An example of such a material is amorphous hydrogenated carbon (a-C:H). It is of technological interest because it can be prepared harder, denser and more resistant to chemical attack than any other solid hydrocarbon [1, 2], which, together with a high degree of transparency to the infrared and histocompatibility, have led to many applications [3, 4]. The macroscopic properties of this material depend critically on the conditions under which it is prepared [5]: forms of a-C:H vary from the soft, polymeric (high hydrogen content with many $–CH_2–$ chains) at one extreme and graphitic (high sp^2 carbon content, low hydrogen content) at the other. Hard or 'diamond-like' a-C:H forms under conditions of intermediate deposition energies, which result in a large degree of cross-linking and structural rigidity, and an intermediate hydrogen content. Over the past few years we have developed a model for the structure of a-C:H based mainly on the results of neutron and x-ray scattering and NMR experiments [6]. In particular, from the high-resolution neutron diffraction data, it was found that the dominant sp^2 carbon-bonding environment is olefinic, rather than graphitic [7]. We now turn our attention to studying the structure of nitrogen-doped a-C:H, i.e. a-C:N:H.

0953-8984/96/264739+12$19.50

a-C:N:H was first prepared in 1982 by Jones and Stewart [8]. The motivation behind the addition of nitrogen to a-C:H primarily stemmed from the possible modifications to its electronic properties, and the possibility of their technological applications. The similar sizes of carbon and nitrogen atoms, coupled with the relative ease of sample preparation, makes doping with nitrogen an obvious choice, although a variety of other dopant atoms have been tried (for example, [8, 9]).

Since that time, much experimental work has been carried out on a-C:N:H. Many studies have been centred on the electronic properties of the material [8–14] and structural investigations have been mainly limited to indirect studies using infrared (IR) and Raman spectroscopies [15–19]. However, limited progress has been made in the determination of the effects of nitrogen inclusion on the atomic structure. Conclusions range from nitrogen addition having no observable effect on the structure [16] to it inducing the formation of sp^2-bonded sixfold ring clusters (graphitic layers) [12].

a-C:N:H is potentially a very important new material: it may form a phase harder than undoped a-C:H, and it is already known that adding nitrogen can lead to an increase in conductivity of three orders of magnitude [8]. With the possible technological applications of these properties, and certainly from a fundamental point of view, it is important to examine the effects of nitrogen incorporation by probing the atomic structure of this material.

Diffraction experiments provide an opportunity of obtaining direct information on interatomic distances and on the average numbers of atoms in each coordination shell. Thus far in the studies of a-C:N:H, these have been limited to electron diffraction [9]. Neutron diffraction has already been established as a powerful technique in the study of amorphous materials (see, for example, [7, 20, 21]), and in particular the pulsed neutron source ISIS at the Rutherford Appleton Laboratory (UK) allows one to obtain high-resolution real-space data, to the extent that it is possible to distinguish sp^1, sp^2 and sp^3 carbon-bonding environments directly [7]. Furthermore, because the neutron, unlike x-rays or electrons, scatters from the nucleus, there is no atomic-number-dependent form factor and the correlations involving hydrogen are also accessible. Conversely, this fact may be exploited in x-ray diffraction where it is possible to obtain a pair distribution function which highlights the correlations which do not involve hydrogen. Therefore, we present complementary neutron and x-ray diffraction data for four samples with a range of compositions from 0 to 10 at.% nitrogen, and examine the effect of nitrogen incorporation on the atomic-scale structure of the material.

2. Experimental details

2.1. Sample preparation

Four samples, one of a-C:H and three of a-C:N:H, were prepared using a saddle-field fast-atom (i.e. neutral particle) source [22, 23] from acetylene and nitrogen precursor gases. The samples were prepared at an effective energy of 800 V and a deposition pressure of $\sim 10^{-4}$ mbar. In order to incorporate nitrogen into the samples, nitrogen gas was simply fed into the source with the acetylene at various flow rate ratios.

The diffraction experiments require samples in the form of powders and this is achieved by depositing the thin films onto a copper substrate, previously cleaned with Ar. Since copper carbide does not readily form, the stresses in the thin film soon cause it to detach from the substrate and as it falls the powder sample is collected.

The compositions of the samples were determined by Carlo–Erba CHN combustion analyses, and the densities were measured using a residual volume technique. However, the

measured bulk density is likely to be less than the microscopic density due to the presence of voids. The results of these measurements are summarized in table 1.

Table 1. Compositional information.

Sample	Mass flow ratio of precursor gases acetylene:nitrogen	C in film (at.%)	N in film (at.%)	H in film (at.%)	Density (g cm^{-3})	Number density (atoms Å^{-3})
1	1:0	77	0	23	1.6	0.1
2	1:1	78	6	16	1.6	0.1
3	1:2	74	8	18	1.6	0.1
4	1:3	71	10	19	1.6	0.1

2.2. Neutron diffraction

The data presented here were collected using the SANDALS diffractometer [24] at the pulsed neutron facility, ISIS at the Rutherford Appleton Laboratory (UK). This instrument is particularly well suited to the study of covalently bonded amorphous materials, allowing the collection of data over a wide dynamic range (∼0.2–50 Å^{-1}). It is also optimized for looking at hydrogenous samples by collecting data only at forward-scattering angles to reduce the effects of inelastic scattering. This is discussed more fully in the data analysis section.

Neutrons are scattered from the sample into fixed-angle detectors (i.e. at a given scattering angle 2θ), where the scattered intensity is measured as a function of time of flight (tof), which can be directly related to momentum transfer. The complete scattering profile is then obtained by combining overlapping spectra from different detector angles. Monitors record the tof spectra of the incident and transmitted beams to provide information on the total neutron cross-section and the intensity:wavelength profile of the incident beam. For each experiment measurements are required for: the sample, the empty sample container, a background without sample or container and a vanadium rod of comparable geometry to the sample and container. The vanadium rod measurement allows the sample scattering to be put on an absolute scale, since vanadium has a well-known and almost entirely incoherent scattering cross-section [25].

Table 2. Weighting coefficients for partial pair distribution functions for sample 4, with $b_C = 6.646$, $b_N = 9.362$ and $b_H = -3.741$ in 10^1 fm.

Sample	CC	CN	CH	NN	NH	HH
4	22.26	4.42	−3.35	0.88	−0.66	0.50

In a neutron scattering experiment the aim is to determine a structure factor, $S(Q)$, where, for an amorphous material (i.e. an isotropic scatterer) [25],

$$S(Q) = 1 + \frac{4\pi\rho}{Q}\int_0^\infty r\ \mathrm{d}r\ [g(r) - 1]\sin(Qr) \tag{1}$$

where ρ is the average number density of atoms in the material, $Q = |\boldsymbol{Q}| = |\boldsymbol{k}_i - \boldsymbol{k}_f|$ is the wavevector transfer associated with the diffraction experiment—for elastic scattering from a liquid or amorphous solid, $Q = (4\pi/\lambda)\sin\theta$, where 2θ is the scattering angle and

λ is the neutron wavelength—and $g(r)$ is called the pair correlation function. $g(r)$ is a measure of the atomic density at a distance r from a given origin atom. The pair correlation function may be obtained by Fourier transformation of the structure factor, which is directly related to the measured neutron scattering intensity. For a tertiary system such as a-C:N:H, there are contributions to the total structure factor from each atom-type pair, i.e. there are six independent contributions which are weighted to give the total structure factor. The corresponding real-space function, the total pair correlation function, $G(r)$, is a weighted combination of the partial pair correlation functions, and is defined (according to the Faber–Ziman formalism [25]) as

$$G(r) = \sum_{\alpha\beta}[c_\alpha c_\beta b_\alpha b_\beta g_{\alpha\beta}(r)] \tag{2}$$

where c_α is the atomic fraction and b_α the coherent scattering length respectively, of element α; and where $g_{\alpha\beta}(r)$ represent the partial terms in $G(r)$, and describe the probability of finding an atom of type β at a distance r from an atom of type α at the origin. The weighting coefficients for sample 4, for example, are given in table 2. The weighting of the partials means that, for this sample, the dominant terms are those arising from CC, CN and CH correlations, with CH and NH correlations appearing as troughs rather than peaks since b_H is negative (due to the π-phase-shift experienced by a neutron on scattering from hydrogen). Note that the CH and HC, NH and HN, etc, terms are equivalent.

The equations above rely on the static approximation [26, 27] being valid, i.e. that the change in the neutron's energy on scattering is small compared to its incident energy. Corrections need to be applied to the data before a structure factor can be generated. The major corrections are for background, container and multiple scattering, attenuation and the effects of inelastic scattering. Full details of these may be found elsewhere [28]. The most problematic step in the analysis procedure is the correction for inelastic scattering. Although the SANDALS instrument has been designed to minimize the effects of this on the experimental data, it is by no means completely eliminated and still has to be corrected for. For hydrogenous materials the simplistic approaches [29] to accounting for this deviation from purely elastic scattering (i.e. deviations from the static approximation) break down because of the low mass and high incoherent cross-section of the hydrogen atom, and an alternative method has to be found. The method adopted here is an empirical one which involves fitting a low-order polynomial through the data to remove the underlying incoherent scattering curve; to first order the effects of inelastic scattering are embedded in this term. The procedure for performing this correction is given in detail elsewhere [30]. There are problems with using this approach, particularly with regard to the quality of the data at very low r-values (below $\sim$1 Å) which may affect correlation amplitudes. Therefore, we expect peak areas, and to a far lesser extent bond distances, for correlations involving hydrogen first coordination shells to be subject to larger uncertainties than pertain to the bulk of the data.

2.3. X-ray diffraction

The data presented here were obtained using standard flat-plate (θ:2θ) transmission diffraction geometry [31] on Station 9.1 at the Daresbury Laboratory Synchrotron Radiation Source, Warrington (UK). Measurements were taken of the sample and of the empty sample cell. The windows of the sample cell are made of Kapton which has a well-known and relatively featureless diffraction pattern. Also, the sample is rotated constantly during the experiment. The diffraction data were normalized to allow for variations in the incident flux, corrected for detector deadtime, beam polarization, background scattering effects

(including those from the sample container), absorption and variation of the illuminated sample volume, with analysis based on that described by Warren [31]. As with the case of neutron diffraction, inelastically scattered x-rays affect the data quite considerably. Again, a method of smooth curve fitting is applied until the data oscillates about the calculated self-scattering profile, which is then subtracted to leave the interference function. From this the structure factor, $S(Q)$, can be obtained. The $S(Q)$ produced is in electron units, and via Fourier transformation to $G(r)$, interatomic distances can be determined. Unlike the neutron diffraction data, the weighting coefficients in the x-ray $G(r)$ are monotonically dependent on the atomic number, Z. Thus, for example, a pair distribution function for a-C:H obtained from x-ray diffraction will approximate to the partial function $g_{CC}(r)$.

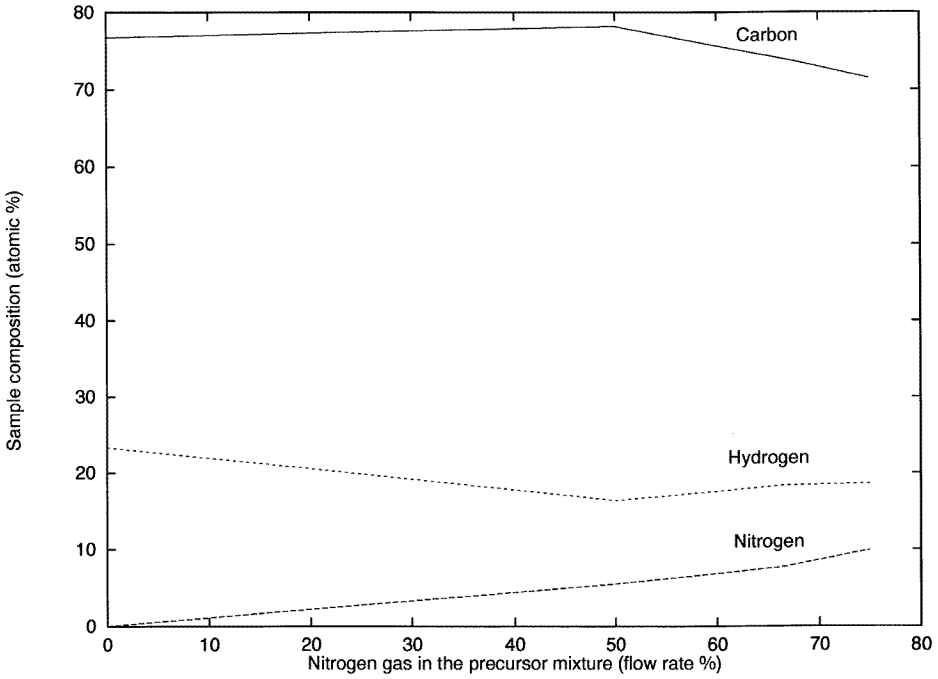

Figure 1. The compositional variation of the four samples.

3. Results and discussion

The changes in sample composition which result form the addition of N are shown in figure 1. Incorporating nitrogen affects the C and H content of the film. This is in agreement with the samples produced by Kaufman and Metin (see [17]) (r.f. magnetron sputtering) where the magnitude of the compositional changes are comparable with this work, but is contrary to the findings of Franceschini *et al* [32] (plasma decomposition of CH_4 and N_2), where the H content remained constant. From our combustion analysis data we observe that the C content decreases steadily with increasing N incorporation, whereas the H content decreases rapidly at low N concentrations and then remains approximately constant as the N content increases to 10 at.%; in going from 0 to 6 at.% N, the H content decreases by $\sim$30% and the C content decreases by only $\sim$1%. So, at low N concentrations the H content

is affected far more than the C content. It is difficult to draw conclusions based on this information alone, particularly given the absence of information concerning the nature of the impacting fragments/species in the deposition process, but it indicates that N may be very effective at etching H from the depositing film, although the effect saturates when the amount of N_2 in the precursor gas reaches 50%.

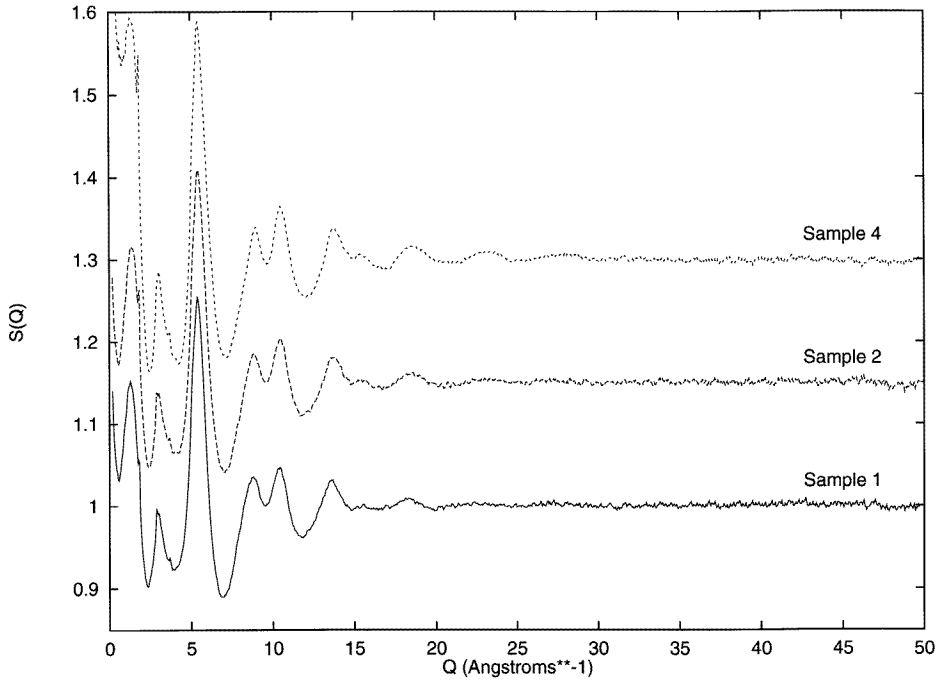

Figure 2. Structure factors for the four samples obtained from neutron diffraction data, where the incoherent scattering has been subtracted (offset for clarity).

Table 3. Results of the Gaussian fitting of the diffraction data.

	First-neighbour peak position (±0.01 Å)		First-neighbour peak width FWHM (±0.01 Å)	Second-neighbour peak position (±0.01 Å)	
Sample	Neutron	X-ray	Neutron	Neutron	X-ray
1	1.46	1.43	0.10	2.45	2.51
2	1.43	1.43	0.10	2.43	2.49
3	—	1.40	—	—	2.47
4	1.42	1.39	0.08	2.43	2.46

Figures 2 and 3, respectively, show the total structure factors and pair correlation functions obtained from the neutron diffraction experiments for the four samples described above. The corresponding x-ray diffraction data are shown in figures 4 and 5. The range of the data in Q-space has a significant effect on the achievable real-space resolution ($\Delta r = 2\pi/Q_{max}$)—the neutron $G(r)$ data, derived from $S(Q)$ spectra, where $Q_{max} \sim 50$ Å^{-1},

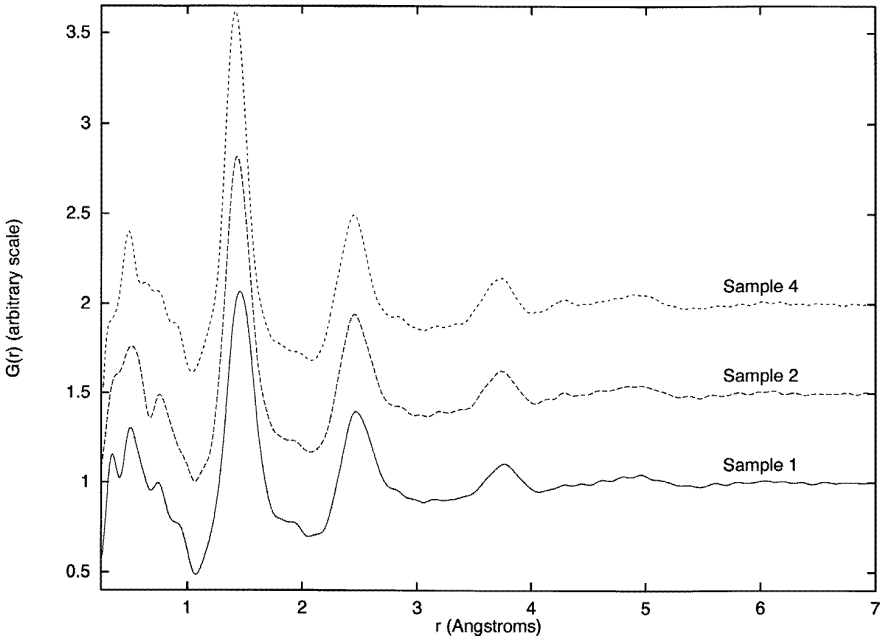

Figure 3. Pair distribution functions for the four samples obtained from neutron diffraction data (offset for clarity).

showing much higher resolution (∼0.1 Å) than that obtained in the corresponding x-ray experiments ($\Delta r \sim 0.4$ Å). However, note that at any given Q-value the Q-space resolution of the x-ray data is greater than that achieved in the neutron diffraction experiments (i.e. only sharp, Bragg-like features associated crystalline inclusions would be more easily detected using the x-ray diffractometer). In addition, in comparing the real-space functions from the neutron and x-ray experiments we note as expected that correlations involving H are not seen in the x-ray data.

In order to obtain quantitative information, such as peak widths and positions, the real-space functions can be fitted with Gaussians, allowing both position and area to vary. For these three-component samples, obtaining accurate values for bond distances is difficult. We have fitted the main first- (∼1.4 Å) and second- (∼2.4 Å) neighbour peaks, together with features either side to improve the accuracy. The results of the Gaussian fitting are given in table 3. For comparison, some of the observed bond lengths for C, N and H are given in table 4 [33].

Consider first of all the total structure factors obtained by neutron diffraction measurements (figure 2). For all of the samples, the oscillations have died away by ∼30 Å^{-1}, indicating a relatively large degree of variation in the short-range ordering (compared, for instance, to that for a prototypical amorphous network such as silica). There are clear differences between the samples with the $S(Q)$s showing shifts in peak positions and changes in peak intensities, particularly in the region 10–25 Å^{-1}. Differences in peak shapes and relative intensities are also observed in the x-ray diffraction data (figure 4). One feature of note in these $S(Q)$s is the single, small Bragg-like peak at 1.9 Å^{-1}; this has been seen in some previous experimental data for a-C:H [34]. This position is consistent with the well-known graphite inter-layer peak (1.92 Å^{-1}), although no other bulk graphite-related peaks

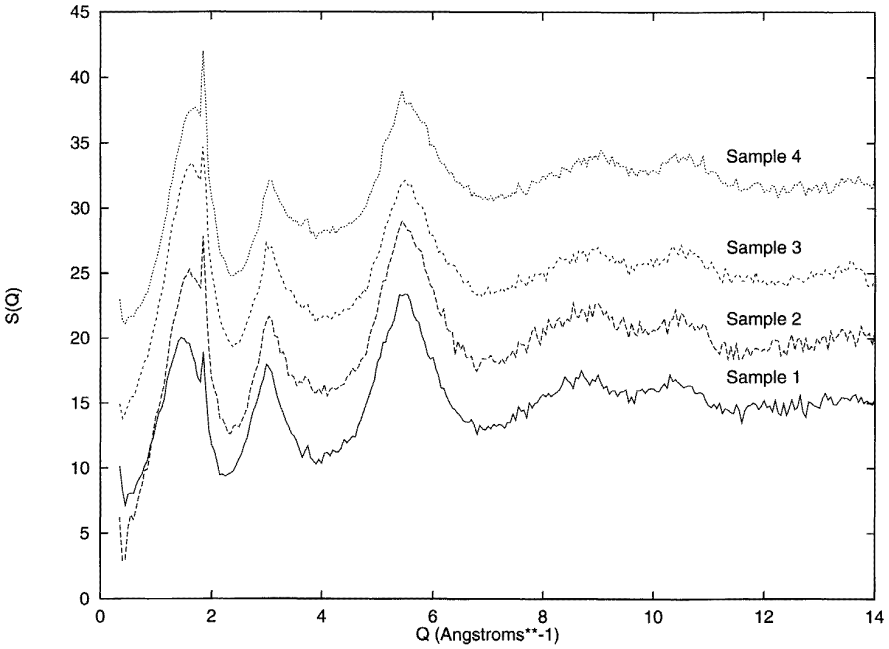

Figure 4. Structure factors for the four samples obtained from x-ray diffraction data (offset for clarity).

are observable in the data. The relative intensity of this peak increases with increasing N content, and it has been found be several workers [12, 13, 14, 35, 36] that the addition of N causes an increase in the number of sp^2 bonds. However, it is hard to generate a definitive statement based solely on the observation of this single isolated peak and we are unable at this time to offer a satisfactory explanation for its presence. Also differences in the scattering intensities are observed in the very-low-Q region (below ~ 2 Å^{-1}) of the neutron diffraction data. Features in this region are due to small-angle scattering which can provide information about the pore size/distribution. In particular, the data for sample 4 show a much higher scattering level than for the other samples. Although this implies that there is more small-angle scattering in sample 4, on the basis of these data, it is impossible to determine the nature of the changes in structure which give rise to this increased intensity. It is noted that similar effects are not observed in the corresponding x-ray data. This is because the internal surfaces of pores which generate the small-angle scattering are likely to be lined with H atoms and, as we have already stated, correlations involving H have a negligible contribution to the structure factor.

In order to understand what some of these differences mean in terms of structural changes, it is necessary to look at the Fourier-transformed data, the total pair correlation functions $G(r)$.

For both the neutron (figure 3) and x-ray (figure 5) real-space functions the achievable resolution of the experimental data is not sufficient for us to observe the different CC, CN and NN bond lengths, but they all merge to form a broad peak at $\sim$1.4 Å. The same is also true for their second-neighbour correlations at $\sim$2.5 Å. (Solid-state NMR data would be most revealing in this context.) For correlations involving hydrogen, the neutron diffraction

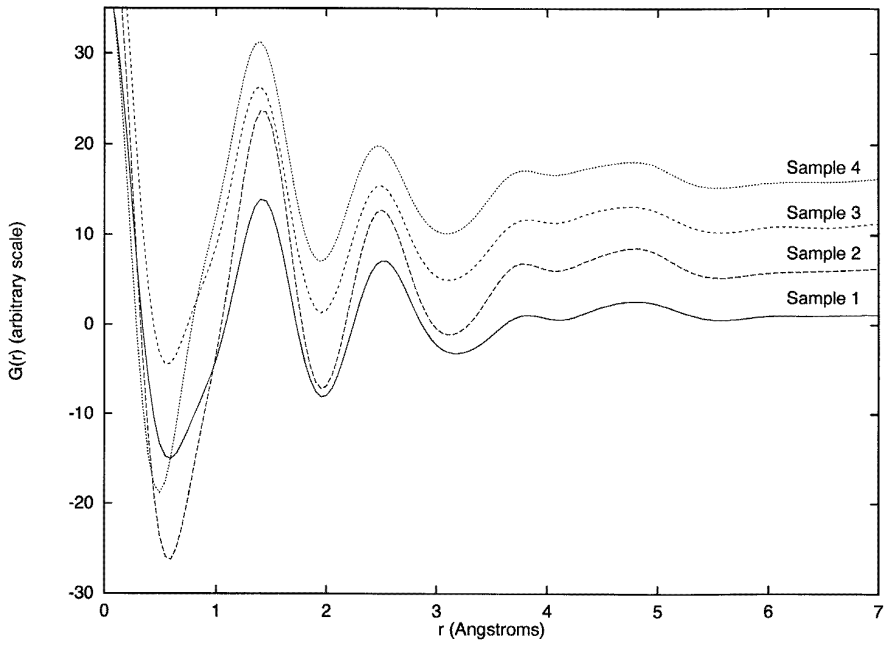

Figure 5. Pair distribution functions for the four samples obtained from x-ray diffraction data (offset for clarity).

data show a definite negative-going region at ∼1.0–1.1 Å, and there is a possibility that some samples show a small H–H peak at ∼0.8 Å, but this is no more significant than other small peaks at lower r-values and therefore cannot be taken as definite evidence for the presence of H_2 molecules as has been observed in previous experimental data [7, 37]. By considering the Gaussian-fitting results (table 2), we may consider in detail the changes in structure that might be occurring. For the a-C:H sample the positions of the first-neighbour CC peak are 1.46 Å and 1.43 Å for the neutron and x-ray data, respectively; all of the bond distances obtained from the x-ray data are consistently shorter than the corresponding values from the neutron data. This may be reflecting the fact that the x-rays scatter from the electron distributions, rather than from the nuclei, which are certainly not spherical in a covalent bond. We take the values from the neutron diffraction data to be closest to the actual bond lengths. The CC peak at 1.46 Å shows little asymmetry and the position is consistent with sp^2 being the dominant carbon-bonding environment. However, we are unable to determine whether the sp^2 environment is olefinic, aromatic or graphitic. If the bonding is graphitic, then the absence of Bragg-like features indicates that it is disordered, i.e. it is *not* microcrystalline. On the low-r side of this peak, the C–H dip is observed at ∼1.1 Å, and on the high-r side (∼1.8 Å) features corresponding to H–C–H (positive) and C–C–H (negative) correlations are seen. The main second-neighbour peak at ∼2.5 Å is due to C–C–C correlations.

Adding nitrogen into the structure does not cause qualitative changes but leads to a shift in the main peak positions and a slight change in the width of the first peak. Taking the values from the neutron data in table 2, we can see that the position of the first peak, which includes CC, CN and NN bond lengths, moves from 1.46 Å (0 at.%N) to 1.43 Å (6 at.% N) to 1.42 Å (10 at.% N). The same decrease in average bond length is seen in the x-ray data,

Table 4. Bond lengths and atomic distances of C, N and H [33]

	Bond length (Å)
sp^3 C–C diamond	1.54
sp^2 C≃C graphite	1.42
sp^2 C≃C benzene	1.395
sp^2 C=C ethene	1.34
sp^3 C–H methane	1.09
sp^2 C–H ethene	1.07
sp^3 H–C–H	1.80
sp^2 H–C–H	1.90
$C(sp^3)$–$N(sp^3)$	∼ 1.47
$C(sp^3)$–$N(sp^2)$	∼ 1.47
$C(sp^2)$–$N(sp^3)$	∼ 1.42
$C(sp^2)$–$N(sp^2)$	∼ 1.36
$C(sp^2)$=$N(sp^2)$	∼ 1.28
C≃N aromatic ring	∼ 1.34
$C(sp^1)$≡$N(sp^1)$	∼ 1.14
sp^3 N–N	1.43
sp^2 N=N	∼ 1.42
sp^2 N≃N	∼ 1.30
sp^3 N–H	1.01
H–H hydrogen	0.75

and also in the electron diffraction data of Davis *et al* [9] for nitrogen-doped tetrahedral amorphous carbon. The fact that the addition of nitrogen hardly affects the shape of the curves implies that that nitrogen is incorporated substitutionally into the network with little impact on the network structure. This decrease in average bond length with increasing N content is consistent with an increase in the number of bonds involving N, which are shorter than CC bonds. However, there may be another change in structure which is contributing to this peak shift. In addition to peak positions, table 2 gives the width of the first peak obtained from the neutron diffraction data (the poorer resolution of the x-ray diffraction data does not warrant extracting this information). Notice that for the highest-N-content sample (sample 4) the width of the first-neighbour peak has decreased compared to that of the a-C:H sample, i.e. the range of bonding environments has decreased. This is surprising when an additional atom type has been introduced into the network. In other studies the addition of N has resulted in an increase in structural order [15, 38] or a decrease in sp^3 C sites [9, 12, 17, 35, 36, 39]. Narrowing of this peak then is consistent with an increase in structural order due to N saturating dangling bonds, but is also consistent with a decrease in the number of sp^3 C–C bonds at ∼1.54 Å.

In addition to this shift in the first-neighbour peak position, the position of the second-neighbour CCC, CCN and CNN correlation peak moves to a slightly smaller r-value as more N is incorporated into the network. This is a result of the decrease in the average first-neighbour bond length. These changes in the first- and second-neighbour peak positions result in a corresponding shift in the average bond angle from ∼114° (for 0 at.% N) to ∼118° (for 10 at.% N). For sample 1 (a-C:H) this again shows that the dominant carbon-bonding environment is sp^2, as an sp^3-dominated structure would have an average bond angle closer to the tetrahedral angle, i.e. 109°, but also shows that there are quite a lot of CCC correlations

involving at least one sp^3 C site. When N is added the bond angle is distorted further to 118°, as a consequence of the lower coordination of N and the shorter average bond length. Although the average bond angle approaches that found in graphite rings, 120°, it is clear that the structure remains disordered and the graphite clusters suggested by Mendoza *et al* [12] are not formed.

There is a third feature which shows a gradual shift in position as N is added: the trough at ∼1.1 Å. The position of this negative feature moves closer to 1.0 Å with increasing N content. If we assume that there are contributions in this region from both CH and NH near-neighbour correlations (CH is observed for sample 1 and CH and NH bands are observed in IR data for similar samples [15, 17, 32]) it is clear that at 10 at.% N the shorter NH correlations dominate over the CH. This is surprising since there are approximately seven times as many C atoms as N atoms available for any H atom to bond to, and indicates a strong preference for the formation of NH bonds over that of CH bonds. In fact, both NH and NH_2 have been observed in IR spectra [15, 17, 32].

Also observed in the IR spectra are C≡N triple bonds [15, 17, 18, 32]. In the diffraction data the presence of C≡N would be seen as a peak at ∼1.14 Å. This is close to the position of the negative CH and NH features; however, a shoulder on the low-*r* side of the first-neighbour peak at approximately this distance can be observed in the data for the sample with the highest N content (sample 4). This provides direct evidence for the presence of C≡N bonds, although only in small quantities. It is reasonable that there are few C≡N bonds if we consider their effect on the network. In this bonding environment N is acting as a network terminator (as H does), so adding a large amount of N as C≡N would disrupt the network and weaken the structure significantly. We have already seen from these data that adding N has no qualitative effect on the network structure and Franceschini *et al* [32] also found no change in either structure or hardness. Therefore, although the C≡N is observed as a strong feature in IR spectra, it is certainly not the dominant bonding environment for N; the intensity of the IR feature is due to the associated transition probability matrix elements.

4. Conclusions

The results presented here show that incorporating nitrogen into an a-C:H network has only a subtle effect on the structure, but the average bond distances are seen to decrease, and, correspondingly, the average bond angle increases. These changes are consistent with the introduction of the shorter bond lengths associated with substitutional CN and NN bonds and a possible conversion of some sp^3 C sites to an sp^2 configuration. However, there is no evidence for the formation of graphitic clusters. There is evidence in the region around 1.0 Å in the data, which suggests that at the highest N concentrations the formation of N–H bonds is favoured over that of C–H bonds, although the bond energies are approximately equal. Also in the sample with the highest N content, C≡N triple bonds are observed directly and shown to be present only in small numbers, indicating that this is not the dominant bonding environment for N.

Acknowledgments

We would like to thank A Fassam (Chemistry, UKC) for carrying out the combustion analysis and D T Bowron for his help and the use of his programs for analysis of the x-ray diffraction data. JKW acknowledges the financial support of the Royal 1851 Commission. The experimental work was supported by the EPSRC.

References

[1] Angus J C, Koidl P and Domitz S 1986 *Plasma Deposited Thin Films* ed J Mort and F Jansen (Boca Raton, FL: Chemical Rubber Company Press) ch 4, p 89
[2] Robertson J 1986 *Adv. Phys.* **35** 317
[3] Lettington A H 1991 *Diamond and Diamondlike Films and Coatings* ed J C Angus, R E Clausing, L L Horton and P Koidl (New York: Plenum) p 481
[4] Aisenberg S and Kimock F M 1989 *Mater. Sci. Forum* **52+53** 1
[5] Robertson J 1991 *Prog. Solid State Chem.* **21** 199
[6] Walters J K and Newport R J 1995 *J. Phys.: Condens. Matter* **7** 1755
[7] Walters J K, Honeybone P J R, Huxley D W, Newport R J and W S Howells 1994 *Phys. Rev.* B **50** 831
[8] Jones D I and Stewart A D 1982 *Phil. Mag.* B **46** 423
[9] Davis C A, Yin Y, McKenzie D R, Hall L E, Kravtchinskaia E, Keast V, Amaratunga G A J and Veerasamy V S 1994 *J. Non-Cryst. Solids* **170** 46
[10] Amir O and Kalish R 1991 *J. Appl. Phys.* **70** 4958
[11] Mansour A and Ugolini D 1993 *Phys. Rev.* B **47** 10 201
[12] Mendoza D, Anguilar-Hernandez J and Contreras-Puente G 1992 *Solid State Commun.* **84** 1025
[13] Veerasamy V S, Amaratunga G A J, Milne W I, Robertson J and Fallon P J 1993 *J. Non-Cryst. Solids* **164–166** 1111
[14] Davis C A, McKenzie D R, Yin Y, Kravtchinskaia E, Amaratunga G A J and Veerasamy V S 1994 *Phil. Mag.* B **69** 1133
[15] Han H and Feldman B J 1988 *Solid State Commun.* **65** 921
[16] Franceschini D F, Achete C A, Freire F L. Beyer W and Mariotto G 1993 *Diamond Relat. Mater.* **3** 88
[17] Kaufman J H, Metin S and Saperstein D D 1989 *Phys. Rev.* B **39** 13 053
[18] Viehland J, Lin S, Feldman B J, Kilgore K and Jones M T 1991 *Solid State Commun.* **80** 597
[19] Li D, Lopez S, Chung Y W, Wong M S and Sproul W D 1995 *J. Vac. Sci. Technol.* A **13** 1063
[20] Johnson P A V, Wright A C and Sinclair R N 1983 *J. Non-Cryst. Solids* **58** 109
[21] Gaskell P H, Saeed A, Chieux P and McKenzie D R 1992 *Phil. Mag.* B **66** 155
[22] Franks J 1984 *Vacuum* **34** 259
[23] Franks J 1989 *J. Vac. Sci. Technol.* A **7** 2307
[24] 1985 *Neutron Scattering Instruments at the SNS* February
[25] Newport R J 1988 *Neutron Scattering at a Pulsed Source* ed R J Newport, B D Rainford and R Cywinski (Bristol: Hilger) ch 13, p 233
[26] Squires G L 1978 *Introduction to the Theory of Thermal Neutron Scattering* (Cambridge: Cambridge University Press)
[27] Gunn J M F 1988 *Neutron Scattering at a Pulsed Source* ed R J Newport, B D Rainford and R Cywinski (Bristol: Hilger) ch 1, p 5
[28] Howells W S, Soper A K and Hannon A C 1989 ATLAS–analysis of lime-of-flight diffraction data from liquid and amorphous samples *Rutherford Appleton Laboratory Report* RAL-89-046
[29] Placzek G 1952 *Phys. Rev.* **86** 377
[30] Turner J Z and Soper A K 1995 *SANDALS Survival Guide* unpublished
[31] Warren B E 1990 *X-ray Diffraction* (New York: Dover)
[32] Franceschini D F, Achete C A and Freire F L 1992 *Appl. Phys. Lett.* **60** 3229
[33] Weast R C (ed) 1987 *CRC Handbook of Chemistry and Physics* 1st student edn (Boca Raton, FL: Chemical Rubber Company Press)
[34] Walters J K, Algar C D, Burke T M, Rigden J S, Newport R J, Bushnell-Wye G, Howells W S and Sattel S 1996 *J. Non-Cryst. Solids* **197** 41
[35] McKenzie D R, Yin Y, Marks N A, Davis C A, Kravtchinskaia E, Pailthorpe B A and Amaratunga G A J 1993 *J. Non-Cryst. Solids* **164–166** 1101
[36] Amarantunga G A J, Veerasamy V S, Davis C A, Milne W I, McKenzie D R, Yuan J and Weiler M 1993 *J. Non-Cryst. Solids* **164–166** 1119
[37] Honeybone P J R, Newport R J, Howells W S, Tomkinson J and Revell P J 1991 *Chem. Phys. Lett.* **180** 145
[38] Li S, Noonan K, Feldman B J, Min D and Jones M T 1991 *Solid State Commun.* **80** 101
[39] Veerasamy V S, Yuan J, Amaratunga G A J, Milne W I, Gilkes K W R, Weiler M and Brown L M 1993 *Phys. Rev.* B **48** 17 954